

Luminosity determination for the pd reaction at 2.14 GeV with WASA-at-COSY*

ZHENG Chuan^{1,2,4,5;1)} M. Büscher^{1,2} P. Fedorets³ V. Hejny^{1,2} H. Ströher^{1,2}
XU Hu-Shan⁴ YUAN Xiao-Hua^{1,2,4}

¹ (Institut für Kernphysik, Forschungszentrum Jülich, 52425 Jülich, Germany)

² (Jülich Center for Hadron Physics, Forschungszentrum Jülich, 52425 Jülich, Germany)

³ (Institute for Theoretical and Experimental Physics, State Scientific Center of the Russian Federation, Bolshaya Cheremushkinskaya 25, 117218 Moscow, Russia)

⁴ (Institute of Modern Physics, Chinese Academy of Sciences, Nanchang Rd. 509, 730000 Lanzhou, China)

⁵ (Institute of Modern Physics, Fudan University, Handan Rd. 220, 200433 Shanghai, China)

Abstract The luminosity for a WASA-at-COSY experiment involving the pd reaction at 2.14 GeV proton-beam energy is determined by the forward pd elastic scattering, which yields an average beam-on-target value of $[5.2 \pm 0.3(\text{stat}) \pm 0.3(\text{syst})] \times 10^{30} \text{ s}^{-1} \text{ cm}^{-2}$. In addition, the forward pd elastic-scattering angular distribution is obtained with four-momentum transfer squared $-t$ between $0.16 (\text{GeV}/c)^2$ and $0.78 (\text{GeV}/c)^2$ at this beam energy, which is compared with other experimental data and the pd double scattering model.

Key words luminosity, pd , elastic scattering, angular distribution, double scattering

PACS 13.75.Cs,

1 Introduction

The WASA detector facility [1], a nearly 4π multidetector system equipped with an internal H_2/D_2 frozen-pellet target [2], is now operated at the COoler SYnchrotron COSY-Jülich [3] which delivers proton and deuteron beams with momenta up to 3.7 GeV/c. It serves for the investigation of hadronic processes and systems, such as light meson production, exotic hadronic states, symmetries and their breaking, following pp , pd and dd reactions [4]. WASA is well suited to detect both charged and neutral decays, *e.g.* of the light scalar mesons $a_0/f_0(980)$ produced in such reactions. A first test measurement has been performed in order to obtain the yet unknown light-scalar production cross sections in $pd \rightarrow {}^3AX$ processes at a beam energy of $T_p = 2.14$ GeV from the measurement of its strong decays. We describe here the luminosity determination for this experiment.

The luminosity is defined as the number of beam particles passing through the target per unit time multiplied by the number of atoms in the target per

unit area. In the case of a stored beam and an internal pellet target, the luminosity can be inferred from the number of beam particles, the beam-revolution frequency, the number of atoms in one pellet, and the beam-pellet overlap factor. The parameters of the COSY beam and the pellet target for this particular experiment are listed in Table 1.

The proton beam in the 184 m long storage ring, circulating with a revolution frequency f related to its energy T_p , has an average beam intensity N_C and a diameter $2R_C$ at the interaction region. The number of beam particles per unit time and area, called current density, is obtained from the formula:

$$j = (N_C f) / (\pi R_C^2) . \quad (1)$$

On the other hand the number of atoms in one D_2 -pellet can be calculated from its radius R_t and density ρ with:

$$N_t(\text{D}) = \frac{4}{3} \pi R_t^3 \rho \frac{n}{M} N_A , \quad (2)$$

where $n = 2$ atoms/molecule for Deuterium, $M \approx 4$ g/mol is its molar mass, and $N_A = 6.022 \times 10^{23}$

Received 2011

* Supported by the Forschungszentrum Jülich including the JCHP-FFE program, the European Community under the FP6 program (Hadron Physics, RII3-CT-2004-506078) & the FP7 program (FP7-INFRASTRUCTURES-2008-1, Grant N.227431), the German BMBF, the China-German CSC-HGF exchange program, the German Research Foundation (DFG) and the National Natural Science Foundation of China (10635080, 10925526)

1) E-mail: zhengchuan@fudan.edu.cn

©2009 Chinese Physical Society and the Institute of High Energy Physics of the Chinese Academy of Sciences and the Institute of Modern Physics of the Chinese Academy of Sciences and IOP Publishing Ltd

molecules/mol is the Avogadro constant. Inserting the numbers from Table 1, the average luminosity for this experiment is estimated as $L \sim 5 \times 10^{30} \text{ s}^{-1} \text{ cm}^{-2}$ which should be regarded as an order-of-magnitude estimate, since the beam diameter and the pellet rate vary as a function of time.

Table 1. Beam and target parameters.

Parameters	Values	Units/remarks
Beam intensity (N_C)	1.7×10^9	particles
Revolution frequency (f)	1.5564 MHz	2.14 GeV
Beam size ($2R_C$)	6 mm	3–6 mm
Current density (j)	9.3×10^{15}	particles/(s·cm ²)
Pellet diameter ($2R_t$)	35 μm	25–35 μm
D ₂ density (ρ)	0.162 g/cm ³	triple point
Atoms/pellet ($N_t(\text{D})$)	1.10×10^{15}	D ₂
Pellet frequency	6 kHz	5–12 kHz
Pellet velocity	70 m/s	60–80 m/s
Pellets in beam	0.5	overlap factor

2 Identification of *pd* elastic scattering

Besides the estimate outlined above, it is useful for luminosity determination to record a monitoring reaction during the experiment, such as elastic scattering for which the corresponding cross sections are well known in dependence of both the beam energy and the scattering angle. In the data acquisition (DAQ) the trigger settings for two charged tracks within WASA were applied to select elastic-scattering events. Both *pd* elastic scattering and *pp* quasi-elastic scattering, with the neutron being a spectator particle, could be recorded by the same trigger condition.

For the scattering processes the data analysis starts with the selection of one charged track in the forward detector (FD, covering emission angles of $\theta = 3\text{--}18^\circ$) and the second one in the central detector (CD, $\theta = 20\text{--}170^\circ$). After a FD-CD time correlation cut, the coplanarity of the two charged tracks is exploited. The corresponding azimuthal-angle correlation is plotted in Fig. 1. For the azimuthal-angle correlated events, the polar-angle correlation of the charged FD and CD tracks is also depicted in Fig. 1. It is seen that most events are located around the *pp* elastic line (determined from a MC simulation) and thus stem from *pp* quasi-elastic scattering. The MC simulations are carried out with the Pluto event generator [6] and the WASA detector simulation package based on GEANT3. The peak around 180° of the azimuthal-angle correlation has a width of $\sigma = 6.9^\circ$ in data, which is reproduced by the simulation of *pp* quasi-elastic scattering, while for *pp* elastic scattering

a much smaller width of $\sigma = 2.0^\circ$ is obtained.

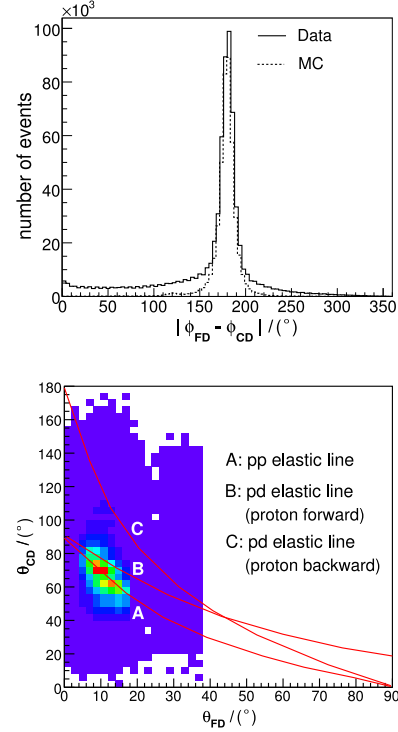


Fig. 1. Angular correlation of two charged tracks for the azimuthal (upper panel) and polar (lower) angles. The dashed line presents the MC simulation of *pp* quasi-elastic scattering from *pd* reaction. Line A depicts the kinematics of *pp* elastic scattering; Lines B and C are for *pd* elastic scattering with the proton emitted in forward and backward direction, respectively.

The *pd* elastic-scattering events, with the proton detected in the FD and the deuteron in the CD, can be identified on top of a huge background from the above mentioned *pp* quasi-elastic scattering. For the charged track in the CD, the ΔE -vs.-momentum distribution is presented in Fig. 2 together with the expected proton and deuteron lines obtained from a MC simulation. A weak cut is applied, which then allows one to extract the *pd* elastic-scattering events from the strongly reduced *pp* quasi-elastic background. For the deuteron candidates the agreement between the polar-angle value measured directly in the CD and the one calculated from the other charged track in the FD is checked on an event-by-event basis. Figure 2 shows that a clear peak of forward *pd* elastic scattering appears around zero angular difference. We did not further analyze the backward *pd* elastic scattering with the deuteron in the FD and the proton in the CD since there are very few events around Line C shown in Fig. 1.

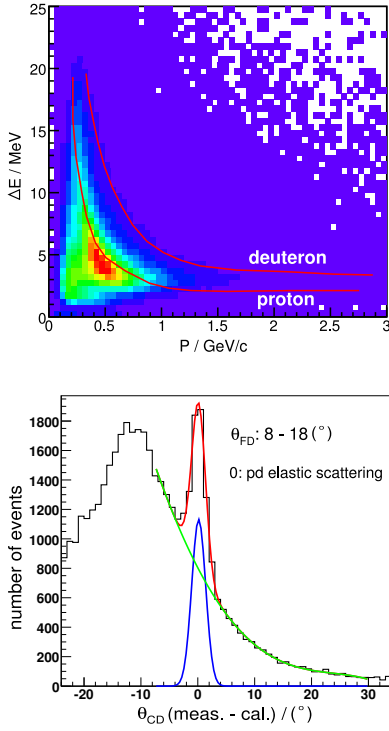


Fig. 2. Upper panel: Energy deposited in the plastic scintillator *vs.* momentum reconstructed in the solenoid field of WASA. Lower panel: Difference of the measured polar angle of the charged track in the CD and the one calculated from the measured polar angle in the FD assuming forward *pd* elastic kinematics. The background under the *pd* elastic-scattering peak has been fitted by a fourth order polynomial and is shown by the green line (color online). The remaining signal is also indicated in the figure by a Gaussian distribution.

3 Normalization of *pd* angular distribution

The normalization of *pd* elastic-scattering angular distribution $(dN/d\Omega)_{\text{lab}}$ to the differential cross sections $(d\sigma/d\Omega)_{\text{lab}}$ is described by the formula:

$$L_{\text{int}} = \left(\frac{dN}{d\Omega}\right)_{\text{lab}} / \left(\frac{d\sigma}{d\Omega}\right)_{\text{lab}}, \quad (3)$$

where L_{int} is the integral luminosity for the corresponding beam time.

The forward *pd* elastic-scattering angular distribution from our data with four-momentum transfer squared $-t$, given in Table 2, is obtained in a polar-angle interval of 1° in the FD with the *pd* elastic-scattering peak observed starting from 8° to 18° in the lab frame. The $-t$ is the Lorentz-invariant momentum transfer ranging from 0.16 (GeV/c)^2 to

0.78 (GeV/c)^2 . The number of *pd* elastic-scattering events is extracted from the number of total events in the gaussian $\pm 3\sigma$ region with the relative area ratio of the gaussian peak to the polynomial background, shown in Fig. 2, and the statistical error is taken from the number of total events and the fitting error of the polynomial background. The geometric acceptance, reconstruction and cut efficiencies have been determined as a whole from the MC simulation for each polar-angle interval as listed in Table 2. In addition, the trigger pre-scaling factor is 2 000 for the first 35 runs and then 4 000 for the later 123 runs. The DAQ lifetime correction is estimated with a relative error 12.4%. Both, the statistical error and the DAQ lifetime-correction error, are listed in Table 2.

Table 2. Forward *pd* elastic-scattering angular distribution at 2.14 GeV from our data. The last column $(dN/d\Omega)_{\text{lab}}$ includes the statistical error of the *pd* elastic-scattering events and the error of the DAQ lifetime correction.

proton, θ_{lab} ($^\circ$)	$-t$ (GeV/c) 2	efficiency (%)	$(dN/d\Omega)_{\text{lab}}$ ($\times 10^6/\text{sr}$)
8.5	0.186	10.4	$5640 \pm 190 \pm 699$
9.5	0.231	42.0	$884 \pm 31 \pm 110$
10.5	0.281	49.3	$532 \pm 24 \pm 66$
11.5	0.336	51.1	$314 \pm 16 \pm 39$
12.5	0.394	51.2	$238 \pm 12 \pm 30$
13.5	0.457	51.6	$175 \pm 9 \pm 22$
14.5	0.523	52.2	$210 \pm 11 \pm 26$
15.5	0.594	52.4	$139 \pm 8 \pm 17$
16.5	0.668	50.2	$138 \pm 8 \pm 17$
17.5	0.745	38.2	$118 \pm 10 \pm 15$

The forward *pd* elastic-scattering differential cross sections from 2.0 GeV data [11] with four-momentum transfer squared $-t$ between 0.35 (GeV/c)^2 and 1.0 (GeV/c)^2 are fitted with the exponential function $a \cdot e^{b(-t)}$, shown in Fig. 3, which has a slope value $b_1 = -1.87 \pm 0.09$, while a slope $b_2 = -1.84 \pm 0.50$ is obtained from fitting our data independently. When the slope value is fixed as $b = -1.87$ for both cases, the fitting procedure gives the coefficient $a_1 = 710 \pm 11 \mu\text{b/sr}$ for 2.0 GeV data and $\tilde{a}_2 = 465 \pm 26 \mu\text{b/sr-pb}^{-1}$ for our data, respectively. Then, a scaling factor is applied to normalize our data to the same height of 2.0 GeV data, which leads to the integral luminosity.

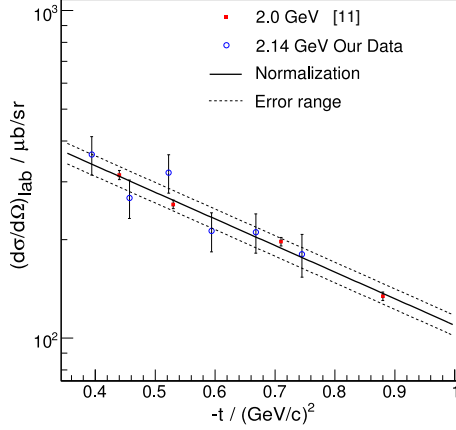


Fig. 3. Normalization of the pd elastic-scattering angular distribution from our data to the differential cross sections from 2.0 GeV data with $-t$ between 0.35 (GeV/c)^2 and 1.0 (GeV/c)^2 . The fit function is an exponential.

The pd elastic-scattering differential cross sections for protons in the forward direction with four-momentum transfer $-t$ less than 1.0 (GeV/c)^2 are plotted in Fig. 4 for proton-beam energies ranging from 0.425 GeV to 11.90 GeV [7–12].

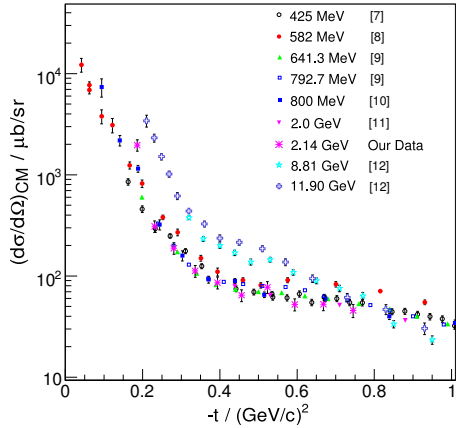


Fig. 4. Compilation of forward pd elastic-scattering differential cross sections *vs.* four-momentum transfer $-t$ including our data after the normalization.

The forward pd elastic-scattering angular distribution can be explained by nucleon-nucleon single and double scattering and their interference for the deuteron as a double scatterer [14, 15]. A further theoretical investigation, which takes the d -state admixture fully into account [13], gives a better description of the shoulder near $-t \approx 0.44 \text{ (GeV/c)}^2$. Our data points are in good agreement with the model calculations around this sensitive region (see Fig. 5) which provides further confidence in the normalization procedure.

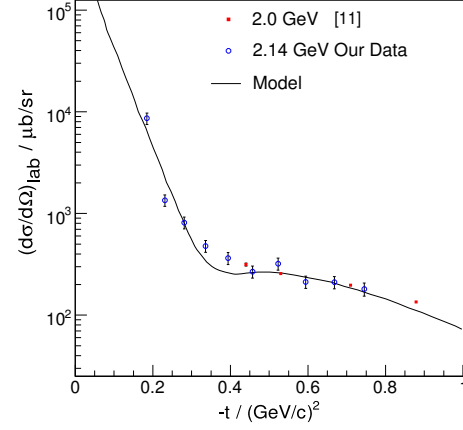


Fig. 5. Comparison of the forward pd elastic-scattering angular distribution available from our data with the model calculation [13] after the normalization.

4 Result and error estimate

The average luminosity in the units of $(\text{s}^{-1}\text{cm}^{-2})$ can be obtained from the integral luminosity divided by the effective beam time, which discards the rest time between the cycles. There are 274 runs in this experiment with a data-taking time of about 80 hours, of which the first 158 runs have the valid trigger condition for the forward pd elastic scattering with the effective beam time 1.19×10^5 seconds. The average luminosity is obtained from this part of the beam time.

In the normalization of the angular distribution, the beam energy difference between our data and 2.0 GeV data is not considered, which could introduce a small correction. The pd elastic-scattering differential cross sections in the lab frame with four-momentum transfer squared $-t$ at 0.44 (GeV/c)^2 are plotted in Fig. 6 for proton-beam energies ranging from 0.425 GeV to 11.90 GeV [7, 9, 11, 12]. After comparing the agreement between data and three kinds of fit functions, the quadratic one is used to estimate the correction factor with a value $c = 1.06 \pm 0.07$ for the differential cross section when the beam energy increasing from 2.0 GeV to 2.14 GeV.

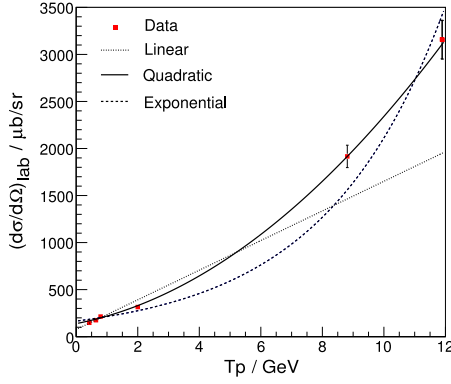


Fig. 6. Fit of pd differential cross sections at the same $-t$ value vs. proton-beam energy. Three kinds of fit functions are compared.

Then, the integral luminosity is deduced as

$$L_{\text{int}}(158 \text{ runs}) = \frac{\tilde{a}_2}{c \cdot a_1} = 0.62 \pm 0.03(\text{stat}) \pm 0.04(\text{syst}) \text{ pb}^{-1}, \quad (4)$$

with the statistical error from \tilde{a}_2 and the systematic error from c and a_1 . This yields the average luminosity during beam-on-target times as

$$L = [5.2 \pm 0.3(\text{stat}) \pm 0.3(\text{syst})] \times 10^{30} \text{ s}^{-1} \text{ cm}^{-2}. \quad (5)$$

Finally, it is possible to estimate the total integral luminosity with the help of another monitoring trigger defined as two charged tracks in the central

detector, which was available during the whole beam time. These two monitoring triggers have almost the same rates after pre-scaling, and their ratio is more or less stable within a relative error of 6.5%. Including the above relative error 12.4% from the DAQ lifetime correction, the ratio of the total integral luminosity to the partial integral luminosity of Eq. 4 is 1.54 ± 0.22 , which yields

$$L_{\text{int}}(274 \text{ runs}) = 0.95 \pm 0.05(\text{stat}) \pm 0.15(\text{syst}) \text{ pb}^{-1}. \quad (6)$$

5 Summary

The aim of this experiment is to measure the light scalar meson $a_0/f_0(980)$ production in $pd \rightarrow {}^3AX$ reactions, while the pd elastic scattering is measured in parallel as a reference reaction to determine the luminosity. As the effective beam time is the same for both aim and reference reactions, the value of the integral luminosity in Eq. 6 is used for the evaluation of the $a_0/f_0(980)$ production cross sections in pd reactions.

We gratefully thank the COSY operators, the technical and administrative staff at the Forschungszentrum Jülich as well as all the members of the WASA-at-COSY collaboration for their support.

References

- 1 Bargholtz C. et al. Nucl. Instr. Meth. A, 2008, **594**: 339—350
- 2 Ekström C. and CELSIUS/WASA Collaboration. Phys. Scripta, 2002, **T99**: 169—172
- 3 Maier R. Nucl. Instr. Meth. A, 1997, **390**: 1—8
- 4 WASA-at-COSY Collaboration. arXiv: nucl-ex/0411038
- 5 Rohdjeß H. et al. arXiv: nucl-ex/0403043
- 6 Fröhlich I. et al. PoS ACAT2007: 076; arXiv: nucl-ex/0708.2382
- 7 Booth N.E. et al. Phys. Rev. D, 1971, **4**: 1261—1267
- 8 Boschitz E.T. et al. Phys. Rev. C, 1972, **6**: 457—466
- 9 Gülmez E. et al. Phys. Rev. C, 1991, **43**: 2067—2076
- 10 Winkelmann E. et al. Phys. Rev. C, 1980, **21**: 2535—2541
- 11 Coleman E. et al. Phys. Rev., 1967, **164**: 1655—1661
- 12 Bradamante F. et al. Phys. Lett. B, 1970, **32**: 303—308
- 13 Franco V. and Glauber R.J. Phys. Rev. Lett., 1969, **22**: 370—374
- 14 Franco V. and Glauber R.J. Phys. Rev., 1966, **142**: 1195—1214
- 15 Franco V. and Coleman E. Phys. Rev. Lett., 1966, **17**: 827—830